articles

molecular pharmaceutics

A Pharmacoproteomics Study of the Cancer Cell Line EKVX Using Capillary-LC/MS/MS

Yonghui Wang,[†,‡] Zunyan Dai,[§] Wolfgang Sadee,[§] and William S. Hancock*[,†]

Barnett Institute, Northeastern University, 360 Huntington Avenue, Boston, Massachusetts 02115, and Department of Pharmacology, The Ohio State University, Columbus, Ohio 43210

Received January 10, 2006

Abstract: The chemotherapeutic agent camptothecin, 10-OH (CPT,10-OH), was shown to act synergistically with the epithelial growth factor receptor (EGFR) inhibitor (AG1478) against several transformed cell lines. To study the cellular response to these drugs, the non-small-cell lung carcinoma cell line, EKVX, was treated with these compounds either alone or in combination. We performed a proteomic analysis using capillary-HPLC coupled with electrospray ion trap mass spectrometry (capillary-LC−ESI/MS) of a tryptic digest to obtain a global protein profile of the EKVX cell line and identify changes in protein expression. The combination of AG1478 and CPT,10-OH showed synergistic cytotoxicity and also changed the expression of multiple proteins, while individual treatments showed a lesser effect on protein expression. Thus, the synergistic action of AG1478 and CPT,10-OH was reflected in altered protein profiles, showing that a proteomic analysis can serve to evaluate chemotherapeutic agents and their combinations.

Keywords: Pharmacoproteomics; mass spectrometry; protein expression; biomarker

Introduction

Targeting pathways selective for cancer cells, chemotherapeutic agents are commonly used in cancer therapies, designed to kill cells or arrest cell growth. Representing a promising new class of anticancer drugs, camptothecin (CPT) analogues target topoisomerase I, which is responsible for rearrangement of DNA structure required for cell growth and replication.[1,2] CPT and its analogues have demonstrated activity against ovarian cancer in clinical trials.[3] It has been shown that inhibition of the topoisomerase I may result in apoptosis and cessation of cellular growth.[4]

Another approach involves molecular targeting of enzymes and growth factor receptors involved in cancer cell growth and survival. For example, epithelial growth factor receptor (EGFR) has been identified as a key factor in cell growth and replication.[5,6] Increased activity of signaling pathways associated with EGFR has been implicated in a variety of solid tumors, such as non-small-cell lung cancer.[7] In addition, EGFR protects malignant tumor cells from the cytotoxic effects of both chemotherapy and radiotherapy, contributing

* Author to whom correspondence should be addressed. Mailing address: Barnett Institute, Northeastern University, 360 Huntington Ave., 341 Mugar Building, Boston, MA 02115. E-mail: wi.hancock@neu.edu. Tel: (617) 373-4881. Fax: 617-373-2855.

[†] Northeastern University.

[‡] Current address: Centocor R&D Inc., 145 King of Prussia Rd., Radnor, PA 19087.

[§] The Ohio State University.

(1) Burris, H. A., 3rd; Fields, S. M. Topoisomerase I inhibitors. An overview of the camptothecin analogs. *Hematol. Oncol. Clin. North Am.* **1994**, *8*, 333−355.

(2) Pommier, Y. Camptothecins and topoisomerase I: a foot in the door. Targeting the genome beyond topoisomerase I with camptothecins and novel anticancer drugs: importance of DNA replication, repair and cell cycle checkpoints. *Curr. Med. Chem.: Anti-Cancer Agents* **2004**, *4*, 429−434.

(3) Kollmannsberger, C.; Mross, K.; Jakob, A.; Kanz, L.; Bokemeyer, C. Topotecan—A novel topoisomerase I inhibitor: pharmacology and clinical experience. *Oncology* **1999**, *56*, 1−12.

(4) Chen, B. M.; Chen, J. Y.; Kao, M.; Lin, J. B.; Yu, M. H.; Roffler, S. R. Elevated topoisomerase I activity in cervical cancer as a target for chemoradiation therapy. *Gynecol. Oncol.* **2000**, *79*, 272−280.

(5) Goustin, A. S.; Leof, E. B.; Shipley, G. D.; Moses, H. L. Growth factors and cancer. *Cancer Res.* **1986**, *46*, 1015−1029.

(6) Aaronson, S. A. Growth factors and cancer. *Science* **1991**, *254*, 1146−1153.

10.1021/mp060002b CCC: $33.50
Published on Web 07/22/2006

to chemoresistance. As a result, treatment of cancer cells with EGFR tyrosine kinase inhibitors can promote apoptosis of cancer cells.[8] Among such targeted cancer therapies, AG1478, an EGFR tyrosine kinase inhibitor, has been shown to inhibit cell proliferation and arrest the cell cycle in nasopharyngeal carcinoma cells.[9,10] Moreover, such targeted inhibitors have the potential to act synergistically with conventional cancer chemotherapeutic agents in killing of tumor cells.[11,12] In this study we tested whether a combination of AG1478 (inhibitor) and CPT,10-OH induces apoptosis more efficiently than either agent alone, using a non-small-cell lung carcinoma, EKVX cell line. Moreover, our objective was to test the utility of a proteomics analysis in studying the mechanism involved in synergism between anticancer drugs.

For anticancer therapy, it is critical to determine how a tumor cell responds to a given drug treatment to understand factors contributing to drug sensitivity or resistance. Proteomics provides a way to identify a significant number of target proteins and quantify changes of protein expression levels in cancer cells during a time course of treatment. Proteomics has been widely used to study the drug treatment of various carcinoma cell lines,[13−17] in which the most commonly used proteomic approach was two-dimensional gel electrophoresis (2DGE). While 2DGE is time-consuming and labor-intensive, shotgun sequencing, i.e., LC/MS of the corresponding tryptic digest, allows a higher throughput identification of peptides and the corresponding proteins.[18] In this study, we used shotgun sequencing to obtain a global profiling of the EKVX cell line that was treated with CPT,-10-OH and the EGFR inhibitor AG1478. We identified 491 proteins for the EKVX cell line, with a significant number of cancer-related proteins identified. In addition, we quantitated the differential expression of 16 proteins with the largest changes in abundance. The proteomic results reflect the synergistic action of AG1478 and CPT,10-OH that has been observed in cell growth measurements. Overall, this study indicates that proteomics technology based on shotgun sequencing, using the new linear ion-trap, can play a significant function in drug and biomarker discovery.

Methods

EKVX Cell Culture. EKVX cell line was purchased from the Division of Cancer Treatment and Diagnosis, National Cancer Institute, National Institutes of Health. EKVX cells were cultured in RPMI 1640 medium with L-glutamine, supplemented with 10% fetal bovine serum, 100 units/mL sodium penicillin G, and 100 μg/mL streptomycin. Cells were grown in tissue culture flasks at 37 °C in a 5% CO_2 atmosphere. EGFR inhibitor AG1478 was purchased from Calbiochem (San Diego, CA). Camptothecin, 10-OH (CPT,-10-OH) was obtained from the Developmental Therapeutics Program at NCI (Bethesda, MD).

Combination Index (CI) Determination. Drug potency was performed using a proliferation assay with sulforhodamine B (SRB).[19] Cells (3000−5000 per well) were seeded in 96-well plates and incubated for 24 h. Drugs were added in a dilution series in triplicate wells. After 3 days, incubation was terminated by replacement of the medium with 100 μL of 10% trichloroacetic acid (Sigma, St. Louis, MO), followed by incubation at 4 °C for 1 h. Plates were then washed with water, air-dried, and stained with 100 μL of 0.4% SRB (Sigma) in 1% acetic acid for 30 min at ambient temperature. Unbound dye was washed off with 1% acetic acid. After air-drying and resolubilization of the protein-bound dye in 100 μL of 10 mM Tris-HCl (pH 8.0), absorbance was read in a microplate reader at 570 nm.

The combination index (CI) was calculated according to the equation $CI = d1/D1 + d2/D2$.[20,21] D1 and D2 represent

(7) Amann, J.; Kalyankrishna, S.; Massion, P. P.; Ohm, J. E.; Girard, L.; Shigematsu, H.; Peyton, M.; Juroske, D.; Huang, Y.; Salmon, J. S.; Kim, Y. H.; Pollack, J. R.; Yanagisawa, K.; Gazdar, A.; Minna, J. D.; Kurie, J. M.; Carbone, D. P. Aberrant Epidermal Growth Factor Receptor Signaling and Enhanced Sensitivity to EGFR Inhibitors in Lung Cancer. *Cancer Res.* **2005**, *65*, 226−235.

(8) Herbst, R. S.; Sandler, A. B. Overview of the current status of human epidermal growth factor receptor inhibitors in lung cancer. *Clin. Lung Cancer* **2004**, *6* (Suppl. 1), S7−S19.

(9) Ward, W. H.; Cook, P. N.; Slater, A. M.; Davies, D. H.; Holdgate, G. A.; Green, L. R. Epidermal growth factor receptor tyrosine kinase. Investigation of catalytic mechanism, structure-based searching and discovery of a potent inhibitor. *Biochem. Pharmacol.* **1994**, *48*, 659−666.

(10) Zhu, X. F.; Liu, Z. C.; Xie, B. F.; Li, Z. M.; Feng, G. K.; Yang, D.; Zeng, Y. X. EGFR tyrosine kinase inhibitor AG1478 inhibits cell proliferation and arrests cell cycle in nasopharyngeal carcinoma cells. *Cancer Lett.* **2001**, *169*, 27−32.

(11) Makin, G.; Dive, C. Apoptosis and cancer chemotherapy. *Trends Cell Biol.* **2001**, *11*, S22−26.

(12) Makin, G.; Dive, C. Modulating sensitivity to drug-induced apoptosis: the future for chemotherapy? *Breast Cancer Res.* **2001**, *3*, 150−153.

(13) MacKeigan, J. P.; Clements, C. M.; Lich, J. D.; Pope, R. M.; Hod, Y.; Ting, J. P. Proteomic profiling drug-induced apoptosis in non-small cell lung carcinoma: identification of RS/DJ-1 and RhoGDIalpha. *Cancer Res.* **2003**, *63*, 6928−6934.

(14) Cecconi, D.; Astner, H.; Donadelli, M.; Palmieri, M.; Missiaglia, E.; Hamdan, M.; Scarpa, A.; Righetti, P. G. Proteomic analysis of pancreatic ductal carcinoma cells treated with 5-aza-2′-deoxycytidine. *Electrophoresis* **2003**, *24*, 4291−4303.

(15) Cecconi, D.; Scarpa, A.; Donadelli, M.; Palmieri, M.; Hamdan, M.; Astner, H.; Righetti, P. G. Proteomic profiling of pancreatic ductal carcinoma cell lines treated with trichostatin-A. *Electrophoresis* **2003**, *24*, 1871−1878.

(16) Poland, J.; Urbani, A.; Lage, H.; Schnolzer, M.; Sinha, P. Study of the development of thermoresistance in human pancreatic carcinoma cell lines using proteome analysis. *Electrophoresis* **2004**, *25*, 173−183.

(17) Sinha, P.; Poland, J.; Kohl, S.; Schnolzer, M.; Helmbach, H.; Hutter, G.; Lage, H.; Schadendorf, D. Study of the development of chemoresistance in melanoma cell lines using proteome analysis. *Electrophoresis* **2003**, *24*, 2386−2404.

(18) Hancock, W. S.; Wu, S. L.; Shieh, P. The challenges of developing a sound proteomics strategy. *Proteomics* **2002**, *2*, 352−359.

(19) Skehan, P.; Storeng, R.; Scudiero, D.; Monks, A.; McMahon, J.; Vistica, D.; Warren, J. T.; Bokesch, H.; Kenney, S.; Boyd, M. R. New colorimetric cytotoxicity assay for anticancer-drug screening. *J. Natl. Cancer Inst.* **1990**, *82*, 1107−1112.

the doses of drug 1 and drug 2 alone, required to produce an effect to a specific extent, and d1 and d2 are the doses of drugs 1 and 2 in combination required to produce the same effect. The combined effect of the two drugs could be synergistic (CI < 1), additive (CI = 1), or antagonistic (CI > 1). Since the CI could differ at different levels of growth inhibition, combination indexes were obtained at different concentrations of these two drugs at a fixed ratio (CPT,10-OH/AG1478 = 2). The combination index was plotted against fraction affected (Fa of 0.25 would equal 75% viable cells).

Cell Lysate Preparation. EKVX cells were treated with 16 μM AG1478, 1.34 μM CPT,10-OH individually or in a combined mode for 4 and 12 h. After removal of cell culture medium, the cells were washed with cold phosphate buffered saline (PBS) and scraped off from cell culture dishes in PBS. The cells were then transferred to Eppendorf tubes and centrifuged at 10 000 rpm for 2 min. The cell pellet was resuspended in 100 μL of lysis buffer (1 mM NaF in PBS buffer pH 7.4, 0.5% Na deoxycholate, 1.0% Triton X-100, 1:100 protease inhibitor cocktail (Sigma Aldrich, St. Louis) and 1:100 phosphate inhibitor cocktail II (Sigma Aldrich, St. Louis)) and incubated on ice for 30 min. The supernatant was collected after being centrifuged at 13 000 rpm, 4 °C for 20 min.

Tryptic Digestion. To each cell lysate sample ($\sim$100 μg of total protein), dithiothreitol was added to a final concentration of 5 mM, and the sample was incubated for 1 h at 75 °C. After cooling to ambient temperature, iodoacetamide was added, to a final concentration of 20 mM. The sample was then incubated in the dark for 2 h at ambient temperature. The samples were desalted by a Microcon spin column (10 kDa MWCO) before tryptic digestion. Trypsin (Promega) was added at a 1:100 (w/w) ratio for an overnight digestion at ambient temperature, another two aliquots of trypsin were added on the next day (4 h apart), and then the sample was incubated for 6 h to complete digestion.

LC/MS Conditions. All the LC/MS experiments were performed on an MDLC system (GE Healthcare) with an LTQ ion trap mass spectrometer (ThermoElectron). CapillaryLC was achieved with a reversed phase column (75 μm i.d. $\times$ 20 cm, Magic C18, 5 μm), coupled with a trap column (Peptide Captrap, Michrom Bioresources). The flow rate was maintained at 10 μL/min for sample loading to the trap column and at 350 nL/min for separation. Mobile phases: A, 0.1% formic acid in water; B, 0.1% formic acid in acetonitrile. A gradient was used as follows: the gradient was ramped from 0% B to 35% B in 60 min, then up to 60% B in 15 min and up to 90% B in another 5 min, and finally held at 90% B for 20 min. MS parameters were set as follows: The ion transfer tube was kept at 185 °C; the normalized collision energy was 35% for MS/MS; and the spray voltage was at 2.0 kV. The seven most intense ions were fragmented for MS/MS analysis after each full MS scan. The tandem MS spectra were acquired twice within 30 s and then excluded from future data dependent scans for 2 min.

Protein Identification and Quantification. Protein identification was obtained through a human database (hrapido_all from SwissProt, 11 932 entries, March 8, 2005) search using the SEQUEST algorithm incorporated into the BioWorks software (version 3.1SR1). The SEQUEST algorithm can construct a peptide sequence from an MS/MS spectrum based on the charge state and *m*/*z* value of the fragment ions and then identify the corresponding proteins through database searching. The identification criteria recommended by HUPO were used in our study, i.e., peptides were identified if the peptide has an Xcorr score (>1.9 for +1; >2.2 for +2; >3.75 for +3) with trypsin cleavage specificity at both ends, and additional criteria of ΔCn $\geq$ 0.1 and RSP $\leq$ 4 were applied as well.[22] For single peptide identification of some interesting proteins, manual intepretation of the MS/MS spectrum was performed.

To quantitate the protein expression changes, peak area of the representative peptides (with good quality MS/MS spectra and Xcorr scores) from each protein were compared. The ion chromatogram of each peptide at its *m*/*z* value ($\pm$ 0.5 Da) was first extracted from each LC/MS run. Seven samples (one control and six treated samples) were analyzed consecutively by LC/MS. The whole analysis (from sample preparation to LC/MS analysis) for the seven samples was repeated on a different day. Reproducible retention times (RSD $\leq$ 1.0%) from run to run were observed for all peptides used in this study. The peak areas for the same peptide from replicate runs and different time points were then integrated for comparison. A comparison of quantitation in replicate analyses established an RSD of less than 20%. In this study, the same amount of fetuin was spiked into each sample as an internal standard and the peak areas of three representative fetuin peptides were used to normalize for any variations in peak area measurement from run to run.

SYBR Green RT-PCR. Total RNA from cell lines was isolated using TRIzol (Invitrogen) and further purified by RNeasy Mini Kit (Qiagen). One microgram total RNA was

(20) Chou, T. C.; Talalay, P. Quantitative analysis of dose-effect relationships: the combined effects of multiple drugs or enzyme inhibitors. *Adv. Enzyme Regul.* **1984**, *22*, 27−55.

(21) Topaly, J.; Fruehauf, S.; Ho, A. D.; Zeller, W. J. Rationale for combination therapy of chronic myelogenous leukaemia with imatinib and irradiation or alkylating agents: implications for pretransplant conditioning. *Br. J. Cancer* **2002**, *86*, 1487−1493.

(22) Omenn, G. S.; States, D. J.; Adamski, M.; Blackwell, T. W.; Menon, R.; Hermjakob, H.; Apweiler, R.; Haab, B. B.; Simpson, R. J.; Eddes, J. S.; Kapp, E. A.; Moritz, R. L.; Chan, D. W.; Rai, A. J.; Admon, A.; Aebersold, R.; Eng, J.; Hancock, W. S.; Hefta, S. A.; Meyer, H.; Paik, Y. K.; Yoo, J. S.; Ping, P.; Pounds, J.; Adkins, J.; Qian, X.; Wang, R.; Wasinger, V.; Wu, C. Y.; Zhao, X.; Zeng, R.; Archakov, A.; Tsugita, A.; Beer, I.; Pandey, A.; Pisano, M.; Andrews, P.; Tammen, H.; Speicher, D. W.; Hanash, S. M. Overview of the HUPO Plasma Proteome Project: Results from the pilot phase with 35 collaborating laboratories and multiple analytical groups, generating a core dataset of 3020 proteins and a publicly available database. *Proteomics* **2005**, *5*, 3226−3245.

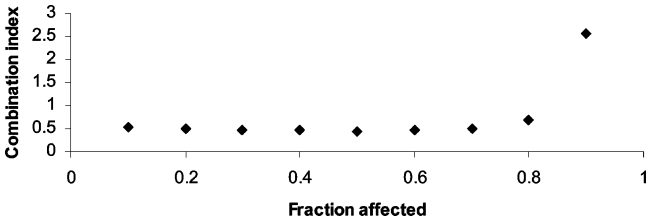

Figure 1. The synergistic anticancer effect of EGFR inhibitor AG1478 and camptothecin 10-OH (CPT,10-OH) in EKVX. The combination index of the two drugs is measured as an indication of synergism.

used for reverse transcription by oligo dT using SUPERSCRIPT First-Strand Synthesis kit (Invitrogen). Primers were designed with Primer Express software (Applied Biosystems, Foster City, CA), and the RT-PCR was performed with the GeneAmp 7000 Sequence Detection system (Applied Biosystems). The primer sequences are as follows: ATP5B-F, 5′-TGAGCATTACGATGTTGCCC-3′, and ATP5B-R, 5′-GGCAATGATATCCTGGAGGGA-3′; CD44-F, 5′-TGCATTGCAGTCAACAGTCG-3′, and CD44-R, AGCTCCATTGCCACTGTTGAT;XRCC5-F,5′-GCCCCCAAAGACAAACCAA-3′, and reverse, 5′-AGCGATGGCAGCTCTCTTAGA-3′; STMN1-RT forward, 5′-CAAATGGCTGCCAAACTGG-3′, and reverse, 5′-TCAGTCTCGTCAGCAGGGTCT-3′. The primer sequences for β-actin were 5′-CCTGGCACCCAGCACAAT-3′ and 5′-GCCGATCCACACGGAGTACT-3′. The PCR was performed in a total volume of 25 μL, with 1× SYBR Green PCR Master mix (Applied Biosystems), 7.5 pmol forward and reverse primers. The PCR reaction was carried out for 40 cycles. For each cycle, the DNA was denatured at 95 °C for 15 s, annealed, and extended at 60 °C for 1 min. The threshold cycle for β-actin was used to normalize the threshold cycle of other genes for comparison between samples. Melting dissociation was performed to evaluate the purity of the PCR product.

Results

Synergistic Induction of Cell Death by AG1478 and CPT,10-OH. EKVX, a human lung epithelial cell line, is one of the NCI-60 cancer cell lines provided for in vitro screening studies. In order to determine the combined effect of the EGFR inhibitor AG1478 and a conventional anticancer drug CPT,10-OH, a non-small-cell lung cancer cell line EKVX was treated with the chemical compounds separately or with a combination at a fixed ratio. The combination index was smaller than 1 for the fraction affected (fa) ranging from 0.1 to 0.8 (Figure 1). This is an indication of synergistic effect for a combination of the two drugs, which is consistent with the previous finding[23] that AG1478 can enhance camptothecin induced apoptosis.

Proteomic Profiling by Shotgun Sequencing (Biomarker Identification). The EKVX cells were treated with either AG1478 or CPT,10-OH, and in a combined mode for 4 h and 12 h. The six treated and control samples were lysed, and the solubilized extract was spiked with fetuin and digested with trypsin. After trypsin digestion, all the samples were analyzed by capillary-LC/MS. In each sample, more than 400 proteins were identified using the SEQUEST algorithm with a stringent criterion, Xcorr ($\geq$1.9 for +1; $\geq$2.2 for +2; $\geq$3.75 for +3). The whole process for the seven samples was repeated in replicate from sample preparation to LC/MS analysis. In these replicate analyses for all EKVX samples (control and treated), a total of 841 proteins were identified with HUPO's criteria, in which 491 proteins were identified with two or more peptides (Table 1). A significant number of cancer-related proteins were identified in this cell line.

Differential Expression of Proteins after Drug Treatment. We compared the six differently treated samples with the control to profile possible target proteins and study the drug effects. As an initial screen, we compared the SEQUEST rank of the same proteins in different samples to identify candidates for peak area quantitation. The candidate list was also constructed using relevant biological information. The measurement of peak areas of multiple selected peptides was used for comparison of protein abundance.[24] The drug treatment resulted in the identification of at least 16 proteins which showed consistent and significant differential quantitation (listed in Table 2).

Figure 2 shows the peak area comparison (a) and MS/MS spectrum (b) of a representative peptide of a down-regulated protein, TD54. Similar information was shown for an up-regulated protein, 143Z, in Figure 3a,b. A good MS/MS spectrum with high Xcorr score was required to establish the peptide identity, and then we used the MS peak area in an extracted chromatogram for comparison of protein abundance. In order to normalize the variations in the sample preparation and LC/MS analyses, we added the same amount of fetuin (bovine) as an internal standard to the cell lysate samples before digestion. Peak areas from three representative fetuin peptides were used for normalization. The variation of the fetuin peptide peak area for all seven samples was less than 20% (see Table 3), which is reasonable considering the potential for differential sample loss during sample preparation and the variability in the LC/MS analysis.

Among the 16 proteins showing the greatest differential quantitation levels after cancer treatment, Table 2 shows that only the known cancer marker, 143Z, was up-regulated after drug treatment. Fifteen other proteins showed down-regulation trends, which includes proteins known to be associated with cancer, such as ATP synthase β chain (ATP5B), tumor protein D54 (TD54), and Stathmin (STMN1).

Synergistic Induction of Proteins by AG1478 and CPT,-10-OH. The greatest changes in protein abundance were

(23) Carson, J. P.; Zhang, N.; Frampton, G. M.; Gerry, N. P.; Lenburg, M. E.; Christman, M. F. Pharmacogenomic identification of targets for adjuvant therapy with the topoisomerase poison camptothecin. *Cancer Res.* **2004**, *64*, 2096−2104.

(24) Wang, Y.; Wu, S. L.; Hancock, W. S.; Trala, R.; Kessler, M.; Taylor, A. H.; Aon, J. C. Proteomic profiling of *Escherichia coli* proteins under high cell density fed-batch cultivation with overexpression of phosphogluconolactonase. *Biotechnol. Prog.* **2005**, *21*, 1401−1411.

Table 1. Total Protein List (with More Than Two Hits)

	protein name		protein name
1	10 kDa heat shock protein, mitochondrial	57	adenylyl cyclase-associated protein 1
2	14-3-3 protein β/α	58	ADP/ATP translocase 2
3	14-3-3 protein ϵ	59	alkaline phosphatase, tissue-nonspecific isozyme
4	14-3-3 protein γ	60	α enolase
5	14-3-3 protein σ	61	α-1 catenin
6	14-3-3 protein θ	62	α-1-antichymotrypsin
7	14-3-3 protein ζ/δ	63	α-1-antitrypsin
8	150 kDa oxygen-regulated protein	64	α-1-antitrypsin-related protein
9	26S proteasome non-ATPase regulatory subunit 4	65	α-2 catenin
10	26S proteasome non-ATPase regulatory subunit 9	66	α-2-HS-glycoprotein
11	28 kDa heat- and acid-stable phosphoprotein	67	α-2-macroglobulin
12	39S ribosomal protein L12, mitochondrial	68	α-actinin 1
13	40S ribosomal protein S10	69	α-actinin 4
14	40S ribosomal protein S11	70	α-endosulfine
15	40S ribosomal protein S12	71	AMP deaminase 2
16	40S ribosomal protein S14	72	amphiphysin
17	40S ribosomal protein S15 (RIG protein)	73	anaphase promoting complex subunit 7
18	40S ribosomal protein S17	74	annexin A1
19	40S ribosomal protein S18 (Ke-3) (Ke3)	75	annexin A11
20	40S ribosomal protein S19	76	annexin A2
21	40S ribosomal protein S21	77	annexin A4
22	40S ribosomal protein S25	78	annexin A5 (placental anticoagulant protein I)
23	40S ribosomal protein S28	79	antigen KI-67
24	40S ribosomal protein S3	80	apolipoprotein A-I
25	40S ribosomal protein S30	81	apolipoprotein B-100
26	40S ribosomal protein S3a	82	arginine/serine-rich splicing factor 10
27	40S ribosomal protein S5	83	aspartate aminotransferase, mitochondrial
28	40S ribosomal protein S8	84	aspartyl/asparaginyl β-hydroxylase
29	40S ribosomal protein SA (colon carcinomalaminin-binding protein)	85	ATP synthase α chain, mitochondrial
		86	ATP synthase β chain, mitochondrial
30	4F2 cell-surface antigen heavy chain	87	ATP synthase D chain, mitochondrial
31	60 kDa heat shock protein, mitochondrial	88	ATP synthase δ chain, mitochondrial
32	60S acidic ribosomal protein P0 (L10E)	89	ATP-dependent DNA helicase II, 80 kDa subunit
33	60S acidic ribosomal protein P1	90	ATP-dependent RNA helicase DDX19B
34	60S acidic ribosomal protein P2	91	barrier-to-autointegration factor
35	60S ribosomal protein L14	92	BH3 interacting domain death agonist (BID)
36	60S ribosomal protein L19	93	brain acid soluble protein 1
37	60S ribosomal protein L22	94	cadherin-releated tumor suppressor homolog
38	60S ribosomal protein L23 (ribosomal protein L17)	95	calcium-activated potassium channel α subunit 1
39	60S ribosomal protein L23a	96	calcium-binding protein 1
40	60S ribosomal protein L27a	97	calcium-binding protein p22
41	60S ribosomal protein L35	98	calcyclin (prolactin receptor associated protein)
42	60S ribosomal protein L36	99	caldesmon (CDM)
43	60S ribosomal protein L6	100	calgizzarin
44	60S ribosomal protein L8	101	calgranulin B
45	78 kDa glucose-regulated protein	102	calmodulin α
46	acetyl-CoA acetyltransferase, mitochondrial	103	calnexin
47	acidic leucine-rich nuclear phosphoprotein 32 family member A	104	calpactin I light chain
48	acidic leucine-rich nuclear phosphoprotein 32 family member E	105	calpain small subunit 1
49	actin, aortic smooth muscle (α-actin-2)	106	calpastatin (Calpain inhibitor)
50	actin, cytoplasmic 1	107	calponin-2
51	activated RNA polymerase II transcriptional coactivator p15	108	calponin-3
52	acyl-CoA-binding protein	109	calreticulin
53	ADAM 2	110	calretinin
54	ADAM 28	111	calumenin
55	ADAM 9	112	cAMP-regulated phosphoprotein 19
56	adenylate kinase isoenzyme 2, mitochondrial	113	caspase recruitment domain protein 6

Table 1 (Continued)

	protein name		protein name
114	CD44 antigen	171	eukaryotic translation initiation factor 3 subunit 4
115	CD50 glycoprotein	172	eukaryotic translation initiation factor 3 subunit 8
116	charged multivesicular body protein 4b	173	eukaryotic translation initiation factor 4 γ 1
117	chemokine-like factor super family member 2	174	eukaryotic translation initiation factor 4B (eIF-4B)
118	chromobox protein homologue 3	175	eukaryotic translationtinitiation factor 4H
119	chromobox protein homologue 5	176	eukaryotic translationtinitiation factor 5A (eIF-5A)
120	cingulin	177	eukaryotic translation initiation factor 5B
121	clathrin heavy chain 1	178	extracellular sulfatase sulf-1
122	clathrin light chain B (Lcb)	179	ezrin-radixin-moesin binding phosphoprotein 50
123	C-Myc binding protein	180	far upstream element binding protein 1
124	cofilin-1	181	far upstream element binding protein 2
125	cofilin-2 (cofilin, muscle isoform)	182	far upstream element binding protein 3
126	coiled-coil domain containing protein 6	183	filamin A
127	cold-inducible RNA-binding protein	184	filamin B
128	collagen α 1(I) chain	185	fk506 binding protein 10
129	collagen-binding protein 2	186	fk506 binding protein 2
130	complement C3	187	fk506 binding protein 3
131	complement component 1, mitochondrial	188	fructose-bisphosphate aldolase AT(lung cancer antigen NT-LU-1)
132	copper=trainsporting ATPase 1	189	fructose-bisphosphate aldolase C
133	Crk-like protein	190	fumarate hydratase, mitochondrial
134	CTP synthase	191	g2/mitotic-specific cyclin B1
135	Cystatin B	192	galectin-1
136	cystic fibrosis transmembrane conductance regulator	193	γ-interferon-inducible protein Ifi-16
137	cytochrome c oxidase polypeptide Va, mitochondrial	194	glia maturation factor beta (GMF-β)
138	cytochrome c oxidase poltpeptide Vb, mitochondrial	195	glucosidase II β subunit
139	cytochrome c	196	glutaredoxin-1
140	D-dopachrome tautomerase	197	glutathione S-transferase P
141	density-regulated protein	198	glyceraldehyde-3-phosphate dehydrogenase, liver
142	deoxyuridine 5′-triphosphate nucleotidohydrolase, mitochondrial	199	gluceraldehyde-3-phosphate dehydrogenase, muscle
143	dermcidin	200	glycine cleavage system H protein, mitochondrial
144	desmin	201	golgi autoantigen, golgintsubfamily A member 2
145	dihydrolipoyldehydrogenase, mitochondrial	202	golgi autoantigen, golgintsubfamily A member 5
146	DNA-binding protein A	203	GPI-anchored protein p137
147	DnaJ homology subfamily C member 8	204	growth factor receptor-bound protein 2
148	dual specificity mitogen-activated protein kinase kinase 7	205	haptaglobin
149	dynactin subunit 2	206	heat shock 70 kDa protein 1
150	electron transfer flavoprotein alpha-subunit, mitochondrial	207	heat shock 70 kDa protein 1L
151	elongation factor 1-α 1	208	heat shock 70 kDa protein 6
152	elongation factor 1-α 2	209	heat shock cognate 71 kDa protein
153	elongation factor 1-β	210	heat shock protein 75 kDa, mitochondrial
154	elongation factor 1-δ	211	heat shock protein HSP 90-α
155	elongation factor 2 (EF-2)	212	heat shock protein HSP 90-β (HSP 84) (HSP 90)
156	elogation factor Tu, mitochondrial precursor (ef-tu) (p43)	213	heat shock protein β-1
157	emerin	214	hemopexin (β-1B-glycoprotein)
158	emilin 1 (elastin microfibril interface-located protein 1)	215	heparin cofactor II
159	endoplasmic reticulum protein ERp29	216	hepatoma-derived growth factor
160	endoplasmin (tumor rejection antigen 1)	217	heterogeneous nuclear ribonucleoprotein A/B
161	endoribonuclease dicer	218	heterogeneous nuclear ribonucleoprotein A1
162	enoyl-CoA hydratase, mitochondrial	219	heterogeneous nuclear ribonucleoprotein D0
163	epithelial protein losttin neoplasm	220	heterogeneous nuclear ribonucleoprotein F
164	epithelial-cadherin	221	heterogeneous nuclear ribonucleoprotein H′
165	epsin-3 (EPS-15 interacting protein 3)	222	heterogeneous nuclear ribonucleoprotein K
166	eukaryotic initiation factor 4A-I	223	heterogeneous nuclear ribonucleoprotein M
167	eukaryotic transition initiation factor I	224	heterogeneous nuclear ribonucleoprotein UP2 (fragment)
168	eukaryotic translation initiation factor 2 subunit 2	225	heterogeneous nuclear ribonucleoprotein A2/B1
169	eukaryotic translation initiation factor 3 subunit 1	226	heterogeneous nuclear ribonucleoprotein U
170	eukaryotic translation initiation factor 3 subunit 10	227	high mobility group protein 1 (HMG-1)

Table 1 (Continued)

	protein name		protein name
228	high mobility group protein 1-like 10 (HMG-1L10)	286	mucin-1(tumor-associated mucin)
229	high mobility group protein 2 (HMG-2)	287	multisynthetase complex auxiliary component p43
230	high mobility group protein 4-like (HMG-4L)	288	myosin light polypeptide 3
231	histone H10 (Histone H1′)	289	myosin light polypeptide 6
232	histone H1.3 (Histone H1c)	290	myosin regulatory light chain 2, atrial isoform
233	histone H1.5	291	myosin regulatory light chain 2, nonsarcomeric
234	histone H1x	292	myosin regulatory light chain 2, smooth muscle isoform
235	histone H2A.m (H2A/m)	293	myosin-11
236	histone H2A.z (H2A/z)	294	myosin-18B
237	histone H4 (H4.1)	295	myosin-7A (myosin VIIa)
238	Hsc70-interacting protein (Putative tumor suppressor ST13)	296	myosin-9
239	hypothetical protein C20orf6	297	myosin-9B
240	integrin α-3	298	myosin-binding protein C, slow-type
241	integrin β-1	299	myotrophin (V-1 protein)
242	inter-α-trypsin inhibitor heavy chain H4	300	myristoylated alanine-rich C-kinase substrate
243	intercellular adhesion molecule-5	301	NADH-ubiquinone oxidoreductase 24 kDa subunit, mitochondrial
244	involucrin	302	NK-tumor recognition protein
245	keratin, type I cuticular Ha1	303	NNP-1 protein
246	keratin, type I cuticular Ha6	304	nonhistone chromosomal protein HMG-14
247	keratin, type I cuticular Ha7	305	nonspecific lipid-transfer protein, mitochondrial
248	keratin, type I cytoskeletal 10	306	NSFL1 cofactor p47
249	keratin, type I cytoskeletal 13	307	nuclear autoantigenic sperm protein
250	keratin, type I cytoskeletal 14	308	nuclear ubiquitous casein and cyclin-dependent kinases substrate
251	keratin, type I cytoskeletal 16	309	nuclear valosin-containing protein-like
252	keratin, type I cytoskeletal 17	310	nuclease sensitive element binding protein 1
253	keratin, type I cytoskeletal 18	311	nucleobindin 1
254	keratin, type I cytoskeletal 19	312	nucleobindin 2
255	keratin, type I cytoskeletal 9	313	nucleolar phosphoprotein p130
256	keratin, type II cytoskeletal 1	314	nucleolin (protein C23)
257	keratin, type II cytoskeletal 2 epidermal	315	nucleophosmin
258	keratin, type II cytoskeletal 5	316	nucleoside diphosphate kinase A (tumor metastatic
259	keratin, type II cytoskeletal 6B	317	nucleoside diphosphate kinase B
260	keratin, type II cytoskeletal 6C	318	nucleosome assembly protein 1-like 1
261	keratin, type II cytoskeletal 7	319	nucleosome assembly protein 1-like 4
262	keratin, type II cytoskeletal 8	320	parathymosin
263	kinectin	321	PDZ and LIM domain protein 1
264	lactoylglutathione lyase	322	peptidyl-prolyl cis-trans isomerase A
265	lamin A/C (70 kDa lamin)	323	peptidyl-prolyl cis-trans isomerase B
266	lamina-associated polypeptide 2, isoforms β/γ	324	peptidyl-prolyl cis-trans isomerase
267	LIM and SH3 domain protein 1	325	peripherin
268	L-lactate dehydrogenase A chain	326	peroxiredoxin 1
269	L-lactate dehydrogenase A-like 6B	327	peroxiredoxin 4
270	L-lactate dehydrogenase B chain	328	peroxiredoxin 5, mitochondrial
271	L-lactate dehydrogenase C chain	329	peroxiredoxin 6
272	lupus La protein	330	peroxisomal biogenesis factor 19
273	lysosome-associated membrane glycoprotein 2	331	PHD finger protein 2
274	macrophage migration inhibitory factor	332	phosphatidylethanolamine-binding protein
275	malate dehydrogenase, mitochondrial	333	phosphoacetylglucosamine mutase
276	mannose-6-phosphate receptor binding protein 1	334	phosphoglycerate kinase 1
277	MARCKS-related protein	335	phosphoglycerate mutase 1
278	membrane associated progesterone receptor component 2	336	plasma protease C1 inhibitor
279	metallothionein-II	337	plectin 1
280	microtubule-actin cross-linking factor 1	338	poly(rC)-binding protein 1
281	microtubule-associated protein 4 (MAP 4)	339	poly(rC)-binding protein 2
282	microtubule-associated protein RP/EB family member 1	340	prefoldin subunit 2
283	mitochondrial 39S ribosomal protein L49	341	prefoldin subunit 4
284	moesin (membrane-organizing extension spike protein)	342	prefoldin subunit 6
285	M-phase phosphoprotein 8 process-associated protein	343	pre-mRNA splicing factor 18

Table 1 (Continued)

	protein name		protein name
344	proactivator polypeptide	399	SH3 domain-binding glutamic acid-rich-like protein 3
345	probable RNA-dependent helicase p68	400	SH3 domain-binding glutamic acid-rich-like protein
346	profilin-1 (profilin I)	401	SH3-domain kinase binding protein 1
347	programmed cell death protein 5	402	signal recognition particle 9 kDa protein
348	programmed cell death protein 8, mitochondrial	403	slit homologue 3 protein
349	proteasome activator complex subunit 1	404	Slp homologue lacking C2 domains-b
350	proteasome activator complex subunit 2	405	small glutamine-rich tetratricopeptide repeat-containing protein A
351	proteasome subunit α type 1	406	sodium/potassium-transporting ATPase α-3 chain
352	protein disulfide-isomerase A3	407	spectrin α chain, brain
353	protein disulfide-isomerase A4	408	spectrin β chain, brain 1
354	protein disulfide-isomerase A6	409	S-phase kinase-associated protein 1A
355	protein disulfide-isomerase	410	splicing factor 3B subunit 2
356	protein FAM3C	411	splicing factor 3B subunit 4
357	protein KIAA0553	412	splicing factor, arginine/serine-rich 1
358	protein KIAA0586	413	splicing factor, arginine/serine-rich 2
359	protein phosphatase 1 regulatory subunit 12A	414	splicing factor, arginine/serine-rich 3
360	protein Plunc (nasopharyngeal carcinoma-related protein)	415	splicing factor, arginine/serine-rich 5
361	protein-glutamine γ-glutamyltransferase	416	splicing factor, arginine/serine-rich 6
362	prothymosin α	417	splicing factor, arginine/serine-rich 7
363	proto-oncogene C-crk	418	SPUF protein
364	putative nucleoside diphosphate kinase	419	Src substrate cortactin
365	putative RNA-binding protein 3	420	stathmin
366	pyruvate carboxylase, mitochondrial	421	stress-70 protein, mitochondrial
367	pyruvate kinase, isozymes M1/M2	422	stress-induced-phosphoprotein 1
368	Rab GDP dissociation inhibitor β	423	striatin-3
369	RAC-α serine/threonine-protein kinase	424	stromelysin-3
370	Ran-binding protein 2	425	structural maintenance of chromosome 1-like 2 protein
371	Ran-specific GTPase-activating protein	426	superoxide dismutase [Mn], mitochondrial
372	Ras-GTPase-activating protein binding protein 1	427	superoxide dismutase
373	Ras-GTPase-activating protein binding protein 2	428	synaptosomal-associated protein 23
374	Ras-related protein Rab-11A	429	talin-1
375	Ras-related protein Rab-20	430	talin-2
376	Ras-related protein Rab-5C	431	tankyrase 1
377	Ras-related protein Rap-1b	432	TATA-binding protein associated factor 2N
378	receptor-type tyrosine-protein phosphatase eta	433	T-cell surface glycoprotein E2
379	Ret finger protein 2 (B-cell chronic lymphocytic leukemia tumor suppressor Leu5)	434	telomerase-binding protein p23
380	reticulocalbin-1	435	tetratricopeptide repeat protein 11
381	reticulocalbin-2	436	TFG protein (TRK-fused gene protein)
382	reticulon 4	437	thioredoxin domain containing protein 12
383	retinal dehydrogenase 1	438	thioredoxin domain containing protein 5
384	ρ GDP-dissociation inhibitor 1	439	thioredoxin
385	ribosome-binding protein 1	440	thioredoxin-dependent peroxide reductase, mitochondrial
386	RNA-binding protein 8A	441	thioredoxin-like protein 2
387	S100 calcium-binding protein A13	442	thyroid hormone receptor-associated protein complex
388	S100 calcium-binding protein A16	443	thyroid receptor interacting protein 11
389	S-100P protein	444	T-plastin (plastin-3)
390	sarcoplasmic/endoplasmic reticulum calcium ATPase 2	445	transcription elongation factor B polypeptide 1
391	semaphorin 3B	446	transcription factor E2F1
392	sentrin-specific protease 1	447	transcription intermediary factor 1-β
393	serine/threonine phosphatase 4 regulatory subunit 1	448	transformation/transcription domain-associated protein
394	serine/threonine protein phosphatase 2A, 48 kDa regulatory subunit B	449	transgelin-2 (SM22-α homologue)
395	serine/threonine protein phosphatase PP1-β catalytic subunit	450	trans-Golgi network integral membrane protein 2
396	serum albumin precursor	451	transitional endoplasmic reticulum ATPase
397	serum amyloid P-component	452	translationally controlled tumor protein
398	SET protein	453	translocon-associated protein α subunit

Table 1 (Continued)

	protein name		protein name
454	transthyretin	473	ubiquinol-cytochrome c reductase complex 14 kDa protein
455	trifunctional purine biosynthetic protein adenosine-3	474	ubiquitin associated protein 2-like
456	triosephosphate isomerase	475	biquitin
457	tropomodulin-3	476	ubiquitin-conjugating enzyme E2 L3
458	tropomyosin 1 α chain	477	ubiquitin-conjugating enzyme E2 N
459	tropomyosin α 3 chain	478	ubiquitin-conjugating enzyme E2-25 kDa
460	tropomyosin α 4 chain	479	UMP-CMP kinase
461	tropomyosin β chain	480	UV excision repair protein RAD23 homologue B
462	tubulin α-1 chain	481	vesicle-associated membrane protein-associated
463	tubulin β-1 chain	482	vesicle-associated membrane protein-associated
464	tubulin β-2 chain	483	vimentin
465	tuftelin	484	vinculin (metavinculin)
466	tumor protein D52	485	voltage-dependent anion-selective channel protein 2
467	tumor protein D53	486	WD-repeat protein 10
468	tumor protein D54	487	Wnt-10a protein
469	tumor-associated calcium signal transducer 1	488	zinc finger and BTB domain containing protein 40
470	tumor-associated calcium signal transducer 2	489	zinc finger protein 217
471	U6 snRNA-associated Sm-like protein LSm7	490	zygote arrest 1 (oocyte-specific maternal effect factor)
472	U6 snRNA-associated Sm-like protein LSm8	491	zyxin (zyxin 2)

Table 2. Changes of Protein Expression from Duplicate Analyses

	ID	protein full name	regulation	fold[a,b]	function (Swiss-Prot)
1	143Z	14-3-3 protein ζ/δ	up	1.7, 2.1	activates tyrosine and tryptophan hydroxylases in the presence of Ca^{2+} and calmodulin-dependent protein kinase II
2	ATPA	ATP synthase α chain	down	1.8, 2.6	produces ATP from ADP in the presence of a proton gradient
3	ATPB	ATP synthase β chain	down	2.4, 1.9	across the membrane
4	BASP	brain acid soluble protein 1	down	2.8, 1.5	n/a
5	CD4	T-cell surface glycoprotein CD4	down	4.3, 2.4	accessory protein for MHC class-II antigen/T-cell receptor interaction; may regulate T-cell activation
6	CD44[c]	CD44 antigen precursor	down	5.6, 2.3	receptor for hyaluronic acid (HA); mediates cell−cell and cell−matrix interactions through its affinity for HA; adhesion with HA plays an important role in cell migration, tumor growth and progression
7	DUT	deoxyuridine 5′-triphosphate nucleotidohydrolase	down	2.4, 2.1	involved in nucleotide metabolism
8	KU86[c]	ATP-dependent DNA helicase II, 80 kDa subunit	down	2.6, 3.8	single stranded DNA-dependent ATP-dependent helicase; the DNA helicase II complex binds preferentially to fork-like ends of double-stranded DNA in a cell cycle-dependent manner
9	PDX1	peroxiredoxin 1	down	2.5, −[d]	involved in redox regulation of the cell; reduces peroxides with reducing equivalents provided through the thioredoxin system but not from glutaredoxin
10	PDX5	peroxiredoxin 5	down	2.3, 2.3	reduces hydrogen peroxide and alkyl hydroperoxides with reducing equivalents provided through the thioredoxin system; involved in intracellular redox signaling
11	STN	stathmin	down	4.8, 3.6	involved in the regulation of the microtubule (MT) filament system by destabilizing microtubules; it prevents assembly and promotes disassembly of microtubules
12	TD54	tumor protein D54	down	2.8, 2.1	n/a
13	COF1	cofilin-1	down	1.9, 2.1	controls reversibly actin polymerization and depolymerization; it is the major component of intranuclear and cytoplasmic actin rods; it has the ability to bind G- and F-actin in a 1:1 ratio of cofilin to actin
14	PRO1	profilin-1	down	2.8, 2.5	binds to actin and affects the structure of the cytoskeleton; at high concentrations, profilin prevents the polymerization of actin, whereas it enhances it at low concentrations; by binding to PIP2, it inhibits the formation of IP3 and DG
15	AAC4	α-actinin 4	down	2.4, 3.0	F-actin cross-linking protein which is thought to anchor actin to a variety of intracellular structures; this is a bundling protein
16	SAP	proactivator polypeptide	down	2.6, 3.0	saposin D is a specific sphingomyelin phosphodiesterase activator

[a] From duplicate analyses. [b] The number is after normalization. [c] The down-regulations of CD44 and KU86 were confirmed by mRNA expression result. [d] Outlier.

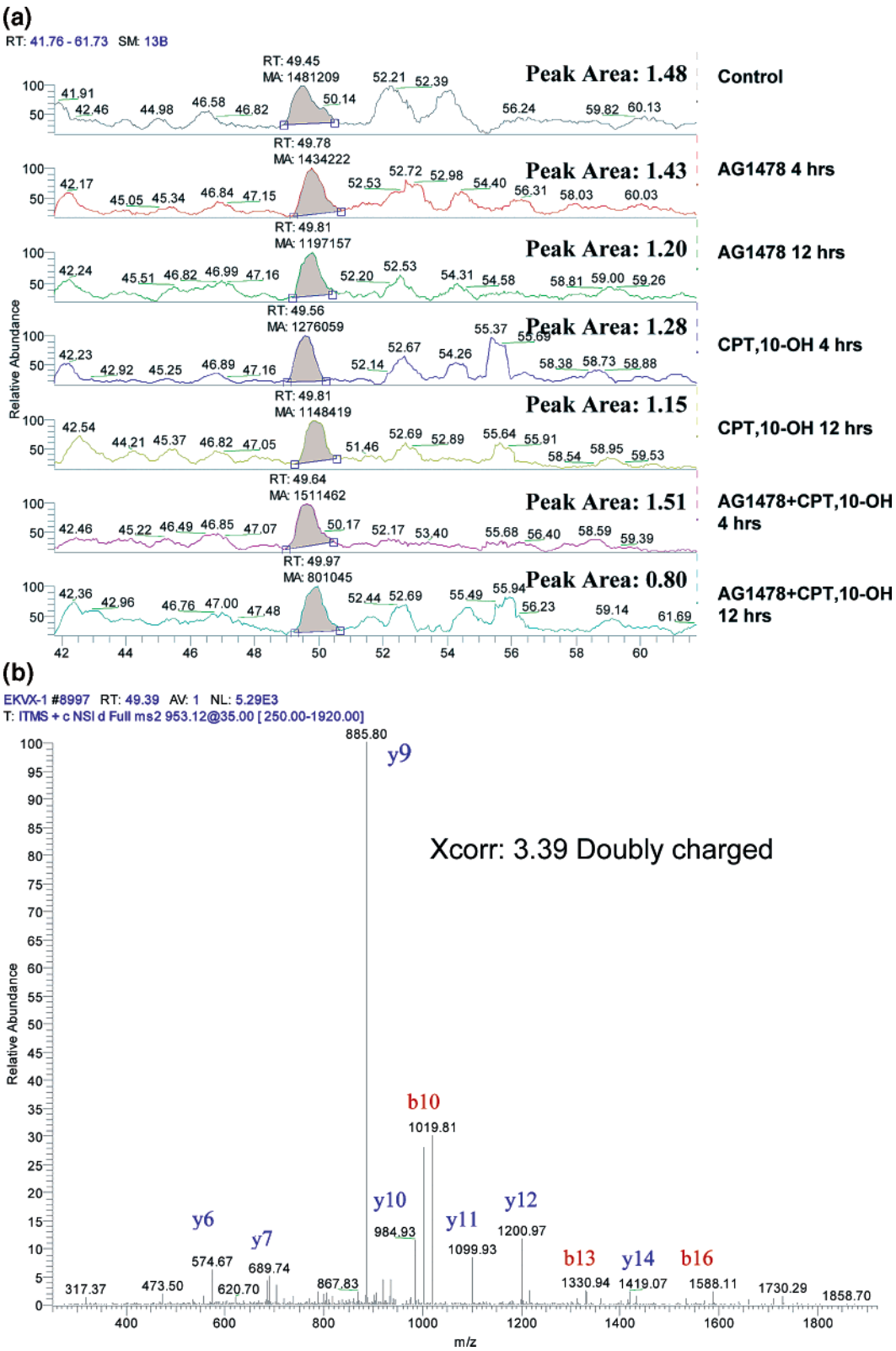

Figure 2. (a) The overlaid extracted ion chromatogram (*m*/*z* 953.0 ± 0.5) of a selected peptide (K.GLLSDSMTDVPVDTGVAAR.T) derived from protein TD54 in the control and treated samples. The residue shown adjacent to the period corresponds to the terminal residue present in the adjacent peptides. (b) The MS/MS spectrum of peptide K.GLLSDSMTDVPVDTGVAAR.T.

observed only after the combination treatment of AG1478 and CPT,10-OH for 12 h (Table 4). Single drug treatment with either AG1478 or CPT,10-OH did not show significant effects on protein expression levels for most of the proteins. These results are consistent with a synergistic function of AG1478 and CPT,10-OH.

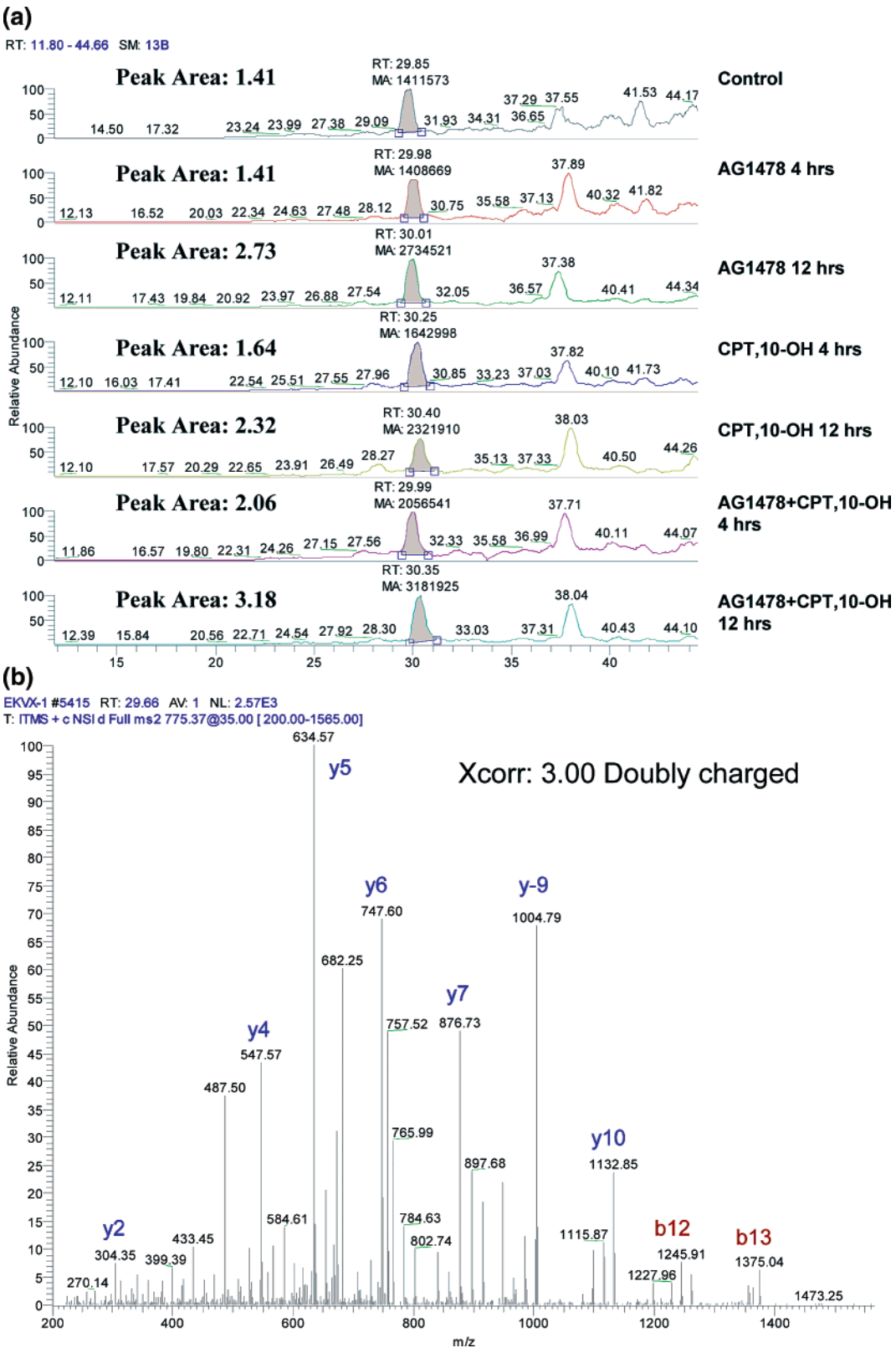

Figure 3. (a) The overlaid chromatogram of a selected peptide (K.SVTEQGAELSNEER.N, *m*/*z* 775.3 ± 0.5) from protein 143Z in the control and treated samples. The residue shown adjacent to the period corresponds to the terminal residue present in the adjacent peptides. (b) The MS/MS spectrum for the peptide K.SVTEQGAELSNEER.N.

To confirm the synergistic induction of gene expression, SYBR green PCR primers were designed for four of the genes: ATP5B, CD44 antigen (CD44), STMN1, and ATP-dependent DNA helicase II, 80 kDa subunit (KU86). After normalization with β-actin, the mRNA level of CD44 and KU86 was 69% and 63% respectively compared to control

Table 3. Peak Area Measurement for Three Fetuin Peptides (A, B, C) in Seven Samples (Seven Consecutive LC/MS Runs), Together with RSD Values

peptide[a,b]	1	2	3	4	5	6	7	av	RSD/%
A	36.0	41.7	40.0	45.2	44.1	33.8	42.8	40.5	10.4
B	30.4	33.7	33.1	36.2	29.2	28.0	33.0	31.9	8.96
C	12.2	9.8	13.5	12.0	12.7	9.2	15.5	12.1	17.7

[a] The unit for peak areas is $\times 10^7$. [b] Sequence of peptides: A, K.TPIVGQPSIPGGPVR.L; B, K.CDSSPDSAEDVR.K; and C, K.QDGQFSV-LFTK.C.

Table 4. Protein Abundance Changes with Different Treatments (Synergistic Effect)[a]

		AG		CPT		AG/CPT	
protein ID	control[b,c]	4 h	12 h	4 h	12 h	4 h	12 h
143Z	1.0	0.7	0.6	0.6	1.1	0.7	2.1
CD4	1.0	0.7	0.6	0.9	0.6	0.8	0.2
CD44	1.0	1.0	0.8	0.9	1.0	0.7	0.2
PDX5	1.0	1.0	1.2	1.1	1.0	1.3	0.4
TD54	1.0	1.0	0.8	0.6	0.9	0.9	0.5

[a] AG-AG1478; CPT-CPT,10-OH. [b] The data were normalized with control values set as 1.0. [c] The RSD for the measurement was approximately 20%, and more of the intermediate time points for either single drug treatment showed a significant difference from control values.

in the AG1478 and CPT,10-OH treated sample for 12 h. The down-regulation of these two genes was less significant in other treatment groups. These results were consistent with the proteomic results. The mRNA expression levels of ATP5B and STMN1 did not change in a significant manner. It has been noted that the level of change in expression profiling studies may not be mimicked in proteomic studies due to a variety of factors. In our study, the presence of protein KU86 has been confirmed by Western blot, but the abundance change was not clear (data not shown).

Discussion

Proteomic Profiling by Shotgun Sequencing (Biomarker Identification). In each sample, we identified more than 200 proteins with HUPO's conservative criteria using the shotgun sequencing approach. By analyzing the seven samples, one control and six treated in replicates, we conservatively identified a total of 491 proteins isolated from EKVX cell line. Since our LC/MS analysis used a data-dependent running mode, after each full MS survey scan, the instrument automatically selected ions from the survey scan for MS/MS fragmentation based on the ion intensity (from high to low). In our method, we set up 7 consecutive MS/MS fragmentations after each full MS scan. Since these samples are very complex and contain a large number of tryptic peptides, different peptide ions could be selected for data-dependent MS/MS scan in replicate LC/MS analyses. Therefore, it is not surprising that we doubled the number of protein identifications by analyzing seven EKVX samples in replicate. In this way, more low abundance proteins were identified and confirmed by repeated identification in replicate analyses. For this lung cancer cell line, a number of cancer-related proteins were identified in our analyses (see Table 1). The fast scan rate and high ion trapping capability of the LTQ instrument significantly improved the efficiency of shotgun sequencing and offered a greater opportunity for putative biomarker discovery.

Differential Expression of Proteins after Drug Treatment. Table 2 lists the 16 proteins that exhibited greatest changes in differential quantitation after treatment and consisted of 1 up-regulated and 15 down-regulated proteins. The table also lists the potential function of each differentially expressed protein. Below we will focus on a discussion of a few of these proteins.

14-3-3 proteins are known to participate in the protein kinase signaling pathway in all eukaryotes, and they function by interacting directly with numerous different target proteins thereby altering their activities. Interactions are generally mediated by phosphorylation of specific binding sites present in the target proteins. The up-regulation of 14-3-3 proteins was also observed in a thermoresistant human carcinoma cell line.[16]

CD44 is a cell surface glycoprotein involved in cell/cell and cell/matrix interactions. Overexpression of CD44 has been linked to the growth and spread of a range of different types of malignancies. The down-regulation of CD44 in our study might suggest an anticancer effect for the drugs used in the treatment.

Integrins are cell adhesion molecules that play an important role in the regulation of angiogenesis. Integrins are the basis for targeted therapy for solid tumors and novel imaging techniques to assess the angiogenic response of tumors.[25] Integrin β 1 is required for the invasive behavior but not for proliferation of squamous cell carcinoma cells in vivo,[26] and the level of expression of β 1 integrins in tumor cells may affect tumor growth.[27] In this study, we found that the integrin β 1 was down-regulated 2-fold after the combination treatment.

ATP-dependent DNA helicase II, 80 kDa subunit (KU86), which is down-regulated 2.6- and 3.8-fold, forms a heterodimer with ATP-dependent DNA helicase II, 70 kDa subunit (KU70), and is involved in the repair of DNA double-strand breaks to maintain the integrity of DNA. It is reported that the suppression of KU70 could sensitize a cell for radio-

(25) Hwang, R.; Varner, J. The role of integrins in tumor angiogenesis. *Hematol. Oncol. Clin. North Am.* **2004**, *18*, 991−1006, vii.

(26) Brockbank, E. C.; Bridges, J.; Marshall, C. J.; Sahai, E. Integrin beta1 is required for the invasive behaviour but not proliferation of squamous cell carcinoma cells in vivo. *Br. J. Cancer* **2004**.

(27) Juliano, R. L. The role of beta 1 integrins in tumors. *Semin. Cancer Biol.* **1993**, *4*, 277−283.

and chemosensitivity.[28] In addition, DNA repair protein XRCC1(XRCC1) overexpression has been shown to play a role in camptothecin resistance.[29] XRCC1 is responsible for the repair of single-strand breaks in DNA typical of those induced by reactive oxygen species and ionizing radiation.

Overall, in this study, we were able to quantify the relative expression levels of some important proteins involved in tumor growth. These findings could be of value in terms of different aspects of drug discovery as well as the monitoring of clinical studies. Table 2 shows a number of microtubular and cytoskeletal proteins, and, as a group, these show consistent changes that could be diagnostic.

Synergistic Function of AG1478 and CPT,10-OH. As we mentioned above, AG1478 and CPT,10-OH may have a synergistic function in cancer therapy. With our proteomic approach, comparing the three different treatments, AG1478 alone, CPT,10-OH alone, and the combined mode, we observed that most of the proteins showed significant changes only with the combination treatment, as shown in Table 4. For instance, protein CD44 was down-regulated about 5-fold with combined treatment for 12 h, but less than 30% down-regulated with either AG1478 or CPT,10-OH. Similar results were observed for 143Z, CD4, and so on. From the results, it was clear that while AG1478 and CPT,10-OH could induce cell apoptosis individually, these agents could have a much greater effect when combined together. This result is not unexpected since both the chemotherapeutic agents and small molecule inhibitors target the control of the cell division and growth. This study suggests that a coordinated combination treatment strategy with drugs that utilize different mechanisms could result in improved therapeutic outcomes.

Conclusions

In conclusion, we performed a proteomic study for the non-small-cell lung cancer cell line, EKVX, treated with an anticancer agent, CPT,10-OH, and an EGFR inhibitor, AG1478. A global profile of EKVX cell line was obtained with 491 proteins identified and the differential quantitation of some important proteins. In addition, a synergistic function of AG1478 and CPT,10-OH was observed in this proteomic study and indicates that the proteomic approach using shotgun sequencing has significant potential in drug discovery studies.

Acknowledgment. The authors would like to thank GE Healthcare and ThermoElectron for instrument support and thank Dr. Shiaw-Lin Wu and Mr. Haven Baker for helpful discussions. Barnett Contribution Number: #873.

MP060002B

(28) Omori, S.; Takiguchi, Y.; Suda, A.; Sugimoto, T.; Miyazawa, H.; Tanabe, N.; Tatsumi, K.; Kimura, H.; Pardington, P. E.; Chen, F.; Chen, D. J.; Kuriyama, T. Suppression of a DNA double-strand break repair gene, Ku70, increases radio- and chemosensitivity in a human lung carcinoma cell line. *DNA Repair* **2002**, *1*, 299−310.

(29) Park, S. Y.; Lam, W.; Cheng, Y. C. X-ray repair cross-complementing gene I protein plays an important role in camptothecin resistance. *Cancer Res.* **2002**, *62*, 459−465.